Journal of Power Sources 190 (2009) 326–330

Contents lists available at ScienceDirect

Journal of Power Sources

journal homepage: www.elsevier.com/locate/jpowsour

Short communication

Enhanced performance of solid oxide fuel cells with Ni/CeO_2 modified $La_{0.75}Sr_{0.25}Cr_{0.5}Mn_{0.5}O_{3-\delta}$ anodes

Xingbao Zhu[a,*], Zhe Lü[a], Bo Wei[a], Kongfa Chen[a], Mingliang Liu[a],
Xiqiang Huang[a], Wenhui Su[a,b,c]

[a] Center for Condensed Matter Science and Technology, Department of Physics, Harbin Institute of Technology, Harbin 150001, PR China
[b] Department of Condensed Matter, Jilin University, Changchun 130022, PR China
[c] International Center for Material Physics, Academia, Shenyang 110015, PR China

ARTICLE INFO

Article history:
Received 27 November 2008
Received in revised form 12 January 2009
Accepted 13 January 2009
Available online 24 January 2009

Keywords:
Solid oxide fuel cells
Perovskite oxide
$La_{0.75}Sr_{0.25}Cr_{0.5}Mn_{0.5}O_{3-\delta}$
Wet impregnation

ABSTRACT

The optimization of electrodes for solid oxide fuel cells (SOFCs) has been achieved via a wet impregnation method. Pure $La_{0.75}Sr_{0.25}Cr_{0.5}Mn_{0.5}O_{3-\delta}$ (LSCrM) anodes are modified using $Ni(NO_3)_2$ and/or $Ce(NO_3)_3$/$(Sm,Ce)(NO_3)_x$ solution. Several yttria-stabilized zirconia (YSZ) electrolyte-supported fuel cells are tested to clarify the contribution of Ni and/or CeO_2 to the cell performance. For the cell using pure-LSCrM anodes, the maximum power density (P_{max}) at 850 °C is 198 mW cm^{-2} when dry H_2 and air are used as the fuel and oxidant, respectively. When H_2 is changed to CH_4, the value of P_{max} is 32 mW cm^{-2}. After 8.9 wt.% Ni and 5.8 wt.% CeO_2 are introduced into the LSCrM anode, the cell exhibits increased values of P_{max} 432, 681, 948 and 1135 mW cm^{-2} at 700, 750, 800 and 850 °C, respectively, with dry H_2 as fuel and air as oxidant. When O_2 at 50 mL min^{-1} is used as the oxidant, the value of P_{max} increases to 1450 mW cm^{-2} at 850 °C. When dry CH_4 is used as fuel and air as oxidant, the values of P_{max} reach 95, 197, 421 and 645 mW cm^{-2} at 750, 800, 850 and 900 °C, respectively. The introduction of Ni greatly improves the performance of the LSCrM anode but does not cause any carbon deposit.

1. Introduction

The substitution of pure hydrogen with economic hydrocarbon fuels such as methane is needed to improve the commercialization of solid oxide fuel cells (SOFCs). Ni/YSZ cermet is the most commonly used anode material for SOFCs, has excellent catalytic properties for H_2 oxidation and acts as a good current collector. However, the Ni/YSZ anodes experience some inherent drawbacks related to sulfur poisoning and carbon deposition when using hydrocarbon fuels and volume instability upon redox cycling [1,2]. For this reason, new anode materials are in demand for SOFCs using hydrocarbon fuels directly. Recently, Ni-free oxides such as ceria [3], titanate [4] and some other perovskite oxides [5] have received increasing attention.

$La_{1-x}Sr_xCrO_3$ (LSCr) [6], which was previously used as a SOFC interconnect, has attracted a great deal of attention due to its excellent stability in both oxidizing and reducing environments at high operating temperatures. However, the low conductivity of the LSCr has limited its application as an anode material through poor electrochemical performance. To improve the conductivity of the LSCr, transition metal elements have been introduced into the Cr-site. Recently, Tao and Irvine [7,8] reported a redox stable $La_{0.75}Sr_{0.25}Cr_{0.5}Mn_{0.5}O_{3-\delta}$ (LSCrM) perovskite-type anode for SOFCs, which have much development potential for high temperature stability and the inhibition of carbon deposits. However, compared to the Ni/YSZ cermet anode, the LSCrM anode does not have adequate electrocatalytic activity, due to its low ionic and electronic conductivity [9,10]. One effective approach for improving the electrochemical performance is incorporating higher ionic or electronic conductive phases into the LSCrM framework, such as $Sm_xCe_{1-x}O_{2-\delta}$ (SDC) [11], $Gd_xCe_{1-x}O_{2-\delta}$ (GDC) [12], Cu [9] and Ni [12]. Previous work has confirmed that wet impregnation is an effective way to deposit nano-sized particles into the pre-established electrode structure [13]. In addition, this technique provides the possibility of effectively avoiding the high temperature interaction between different components in the traditional composite anode.

In the present study, one or more types of SDC, CeO_2 and Ni have been incorporated into the LSCrM structure via a wet impregnation method. The introductions of such fine particles greatly increase effective reaction area and thereby improve the electrocatalytic activity of the LSCrM anode for oxidation reactions. The cell with the Ni/CeO_2 impregnated LSCrM anode exhibited desirable performance using either hydrogen or methane as the reductant.

---

[*] Corresponding author. Tel.: +86 451 86418420; fax: +86 451 86412828.
E-mail addresses: zhuxingbao008@163.com (X. Zhu), lvzhe@hit.edu.cn (Z. Lü).

0378-7753/$ – see front matter © 2009 Elsevier B.V. All rights reserved.
doi:10.1016/j.jpowsour.2009.01.035

2. Experimental

2.1. Electrode and electrolyte preparation

The anode material $La_{0.75}Sr_{0.25}Cr_{0.5}Mn_{0.5}O_{3-\delta}$ was prepared using a combustion synthesis technique [14]. The starting materials were $Cr(NO_3)_3 \cdot 9H_2O$ (99%), $Sr(NO_3)2$ (99.5%), $Mn(NO_3)_2$ solution (A.R.), La_2O_3 (99.5%), citric acid (99.5%), versene acid (>99.5%) and ammonia (A.R.). Before weighing, the La_2O_3 was fired at 1000 °C for 3 h to decompose the carbonates and remove the water adsorbed from air. In the final solution, the molar ratio of versene acid/metal cations/citric acid was 1:1:1.5. The temperature of water-bath was hold at 80 °C, and the pH value of solution was adjusted to 7 with ammonia. The dark purple gel was heated at 150 °C for 6 h and then calcined at 1000 °C for 10 h in air. The single phase LSCrM powders were confirmed by X-ray diffraction (XRD, Bede Scientific D^1, Japan), using Cu Kα radiation ($\lambda = 0.15418$ nm). The well-sintered YSZ electrolyte pellets (relative density >98%) was prepared by pressing 8 mol.% yttria-stabilized zirconia powders (Building Material Science Academy of China) at a pressure of about 200 MPa and sintering at 1400 °C for 4 h.

2.2. Full cell fabrication and characterization

The LSCrM powders were mixed with terpilenol (A.R.) and ethyl cellulose (A.R.) to form a slurry and then coated on sintered YSZ pellets. The LSCrM/YSZ bi-layer was sintered at 1200 °C in air for 2 h to form a porous anode. The thickness of the anode after sintering was 10 μm and the effective electrode area was 0.1 cm^2. $La_{0.8}Sr_{0.2}MnO_{3-\delta}$ (LSM) slurry was coated on the other side of the YSZ electrolyte, followed by sintering at 1100 °C for 2 h. Then the YSZ electrolyte-supported SOFC using LSCrM as anode and LSM as cathode was obtained. In order to improve the ionic conductivity and catalytic activity of the perovskite electrode materials, the LSCrM anodes were impregnated with one or more solutions of $Ni(NO_3)_2$, $Ce(NO_3)_3$ and $Ce_{0.8}Sm_{0.2}(NO_3)_x$, while the LSM cathodes of all cells were impregnated with $Ce_{0.8}Sm_{0.2}(NO_3)_x$ solution followed by firing at 950 °C for 1 h. To avoid a gradient of doped ion across the thickness of the electrode, the process of impregnation was carried out in vacuum conditions [15]. Silver paste (DAD-87, Shanghai Research Institute of Synthetic Resins) was used as the current collector. A four-probe method was used to test the fuel cells, in which dry H_2 or CH_4 was used as fuel and stationary air or flowing oxygen as oxidant. The electrochemical measurements were performed over the temperature range 700–850 °C by an SI 1287 electrochemical interface and an SI 1260 impedance analyzer (Solartron Instruments, Hampshire, UK). A scanning electron microscope (SEM, Hitachi S-570, Japan) was used to analyze the microstructure of the cells.

3. Results and discussion

As shown in Fig. 1(a), for the fuel cell using a pure-LSCrM anode, the maximum power density (P_{max}) at 850 °C was 198 mW cm^{-2} when dry H_2 and air were used as fuel and oxidant, respectively. When the fuel was changed to CH_4, the P_{max} was 32 mW cm^{-2} at 850 °C, as shown in Fig. 1(b).

The wet impregnation method was then employed to improve the performance of the pure-LSCrM anode. SDC was used to improve the ionic conductivity of the pure-LSCrM anode. After the pure-LSCrM anode was impregnated with 6.5 wt.% of SDC, the P_{max} was enhanced from 198 to 400 mW cm^{-2} for H_2 at 850 °C, as shown in Fig. 1(a). For CH_4 fuel, the improvement was also obvious, from 32 to 75 mW cm^{-2}, as shown in Fig. 1(b). The test results given above indicate that the introduction of the SDC leads to a significant enhancement of the performance of the LSCrM anode. That is because the sub-micrometer-sized ionic conducting phase SDC greatly increases the number of reaction sites and then improves the electrocatalytic activity of LSCrM anode for the oxidation reaction [16].

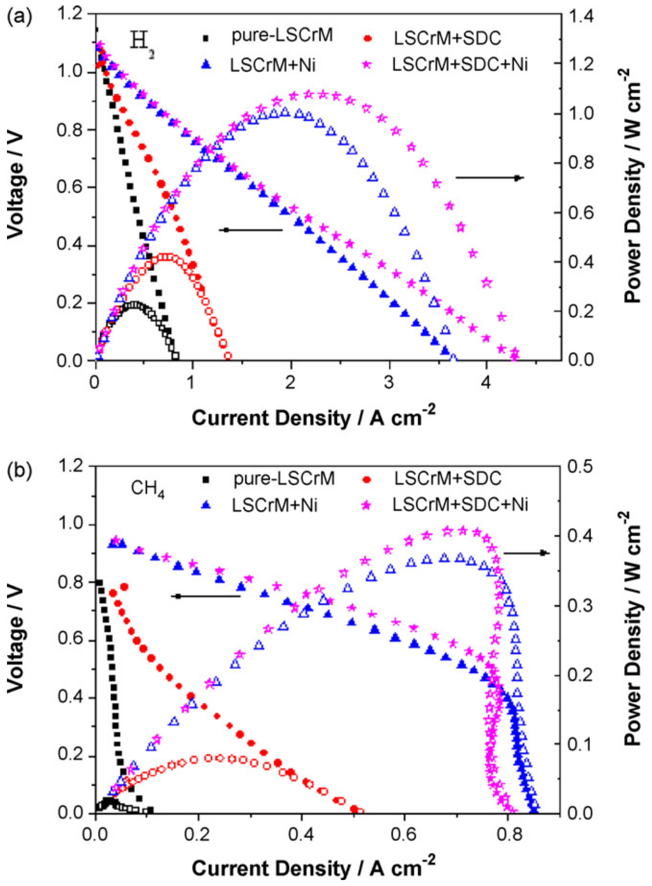

Fig. 1. The P_{max} at 850 °C in (a) dry H_2 and (b) dry CH_4 for the YSZ-supported single-cells using LSCrM-based anodes.

Ni is the most practical catalyst for the oxidation of H_2 and plays a key role in Ni/YSZ anode performance. However, Ni is also the major cause of carbon deposits in the Ni/YSZ anode. A number of studies have suggested that LSCrM can effectively inhibit carbon deposition. Here, we have examined the possibility of using the advantages of Ni and LSCrM. Ni was incorporated into the LSCrM anode to improve the catalytic activity. After the pure-LSCrM anode was impregnated with $Ni(NO_3)_2$ solution, the P_{max} of the cell using LSCrM (89.2 wt.%) + Ni (10.8 wt.%) anode reached 1003 and 362 mW cm^{-2} in dry H_2 and CH_4 at 850 °C, respectively (Fig. 1). The P_{max} of the cell using the Ni modified LSCrM anode is 2.5 and 5 times higher than that of the cell using the LSCrM (93.5 wt.%) + SDC (6.5 wt.%) anode with dry H_2 and CH_4, respectively. These results strongly confirm the catalytic activity of the Ni.

Further, the Ni and SDC were both incorporated into the pure-LSCrM anode. In order to clarify the different contributions of Ni and SDC on the cell performance, several single-cells were prepared and tested under the same fabrication and operating conditions. As described in Fig. 1(a): for the LSCrM (93.5 wt.%) + SDC (6.5 wt.%) anode, the P_{max} was 400 mW cm^{-2} at 850 °C, when H_2 was used as fuel and air as oxidant; under the same conditions, the value for the LSCrM (85.2 wt.%) + SDC (6.2 wt.%) + Ni (8.6 wt.%) anode was 1100 mW cm^{-2} (about 175% increase). The data imply that the introduction of Ni improves the performance more significantly compared with that of SDC only. In contrast, there was a little

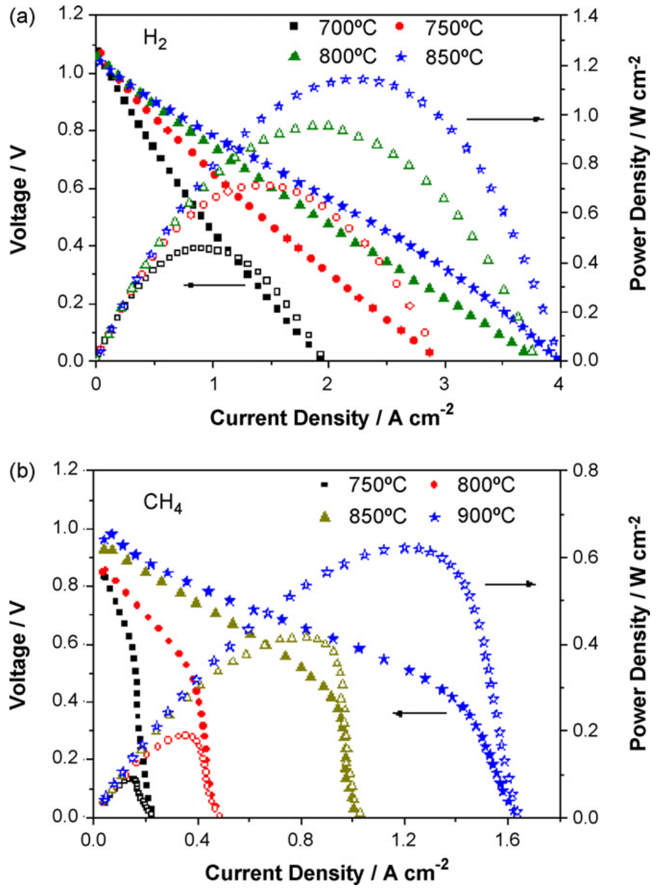

Fig. 2. Full cell performance with LSCrM + Ni + CeO_2 as the anode at different temperatures. The fuel gas was (a) dry H_2 and (b) dry CH_4.

enhancement with the introduction of the SDC particles into the LSCrM + Ni anode (about 10% increase), as shown in Fig. 1(a). It could be concluded that Ni plays a primary role in promoting the performance of the LSCrM-based anode and it is an excellent catalyst for the oxidation of H_2, as described elsewhere [17].

For the oxidation reaction of H_2, the catalytic activity of SDC is lower than that of Ni. However, SDC is also a crucial component of the LSCrM-based composite anodes. When CH_4 was used as a fuel, the P_{max} of the cell using the LSCrM (89.2 wt.%) + Ni (10.8 wt.%) anode without SDC was 362 cm^{-2} at 850 °C, as shown in Fig. 1(b). The introduction of SDC (6.2 wt.%) leads to an obvious enhancement of the cell performance with a P_{max} of 402 mW cm^{-2}. The catalytic effect of adding SDC into the LSCrM + Ni anode is also demonstrated for the oxidation of hydrocarbon fuels. The enhancement of the cell performance is a result of the synergistic effect of Ni and SDC.

The study by Kurokawa et al. has confirmed that the catalytic activity of Sm-doped CeO_2 for hydrocarbon oxidation was lower than that of undoped CeO_2 [18]. When the CeO_2 was used instead of SDC, the cell with the LSCrM (85.3 wt.%) + Ni (8.9 wt.%) + CeO_2 (5.8 wt.%) anode exhibited the best performance, with a P_{max} of 1135 mW cm^{-2} in H_2 at 850 °C, as shown in Fig. 2(a). When the oxidant was changed to O_2 the value rose to about 1450 mW cm^{-2} at 850 °C, which is comparable to that of the Ni/YSZ cermet anode. When dry CH_4 was used as fuel and air as oxidant, the P_{max} of the cell reached 95, 197, 421 and 645 mW cm^{-2} at 750, 800, 850 and 900 °C, respectively (Fig. 2(b)). The P_{max} of the cell using LSCrM + Ni + SDC anode were 1100 and 402 mW cm^{-2} in dry H_2 and CH_4 at 850 °C, respectively, as shown in Fig. 1. There was a slight improvement of the cell performance when the SDC was changed to CeO_2. The importance of CeO_2 in catalysis can be understood from its oxygen storage and release properties. CeO_2 can oxidize a molecule by losing oxygen atoms, with reduction of CeO_2 at the surface. At the same time, oxygen vacancies are formed and the cerium ions are reduced from the +4 state to the +3 state. The reduced CeO_2 can promote reduction of molecules through uptake of oxygen atoms from the molecules by the surface [19]. However, for the Sm-doped CeO_2, Sm^{3+} has taken the place of Ce^{3+}, and it is logical to assume that the Sm^{3+} doping is equivalent to partial reduction of the oxide. The redox of CeO_2 is relatively facile, but for the Sm-doped CeO_2, the presence of the Sm^{3+} constrains the transformation between Ce^{4+} and Ce^{3+} and weakens the oxygen storage capacity of CeO_2 [20]. That is the reason why the catalytic activity of Sm-doped CeO_2 was lower than that of undoped CeO_2.

Fig. 2(a) also shows that the OCV values of the YSZ electrolyte-supported SOFC in dry H_2 are 1.113, 1.105, 1.097 and 1.088 V at 700, 750, 800 and 850 °C, respectively, indicating that a gas tight YSZ pellet is formed by sintering at 1400 °C for 4 h. The OCV of the cell became lower when the fuel was changed to dry CH_4, as shown in Fig. 2(b), which is because the catalytic oxidation of methane is much more difficult than that of H_2 [21]. The introduction of the CeO_2 and Ni into the pure-LSCrM anode can effectively enhance the value of OCV (Fig. 1). This is ascribed to the improvement in the conductivity and catalytic activity of the anode.

As shown in Fig. 2(b), the *I*–*V* plots represent sharply negative curvatures and the current density is limited in the relatively high current density region. This phenomenon cannot be easily considered as the usual concentration polarization concerning the

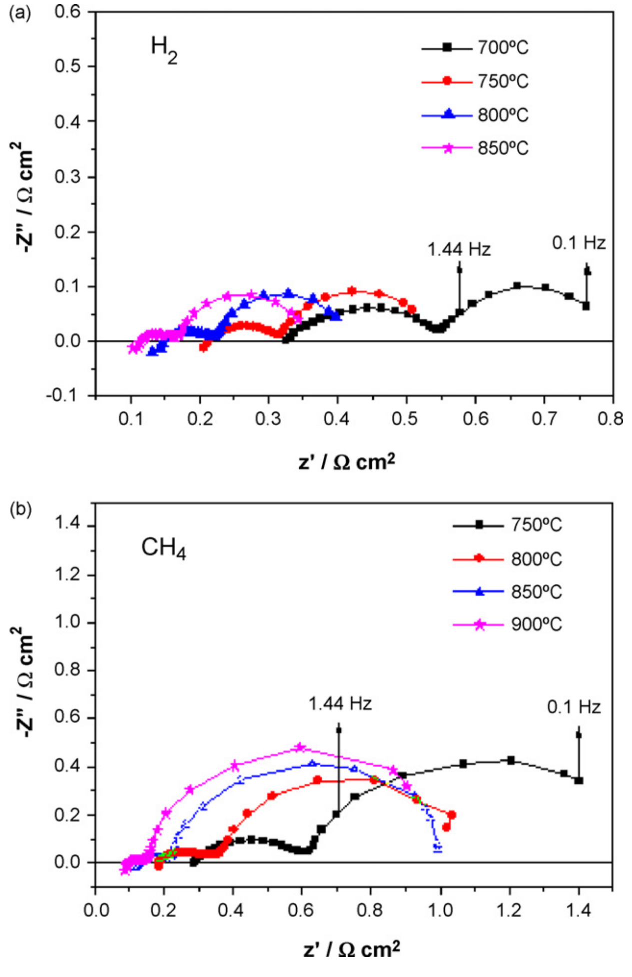

Fig. 3. The impedance curves for a SOFC with the electrolyte-supported system LSCrM + Ni + CeO_2/YSZ/LSM + SDC at different temperatures using (a) dry H_2 and (b) dry CH_4 as fuel under the open circuit.

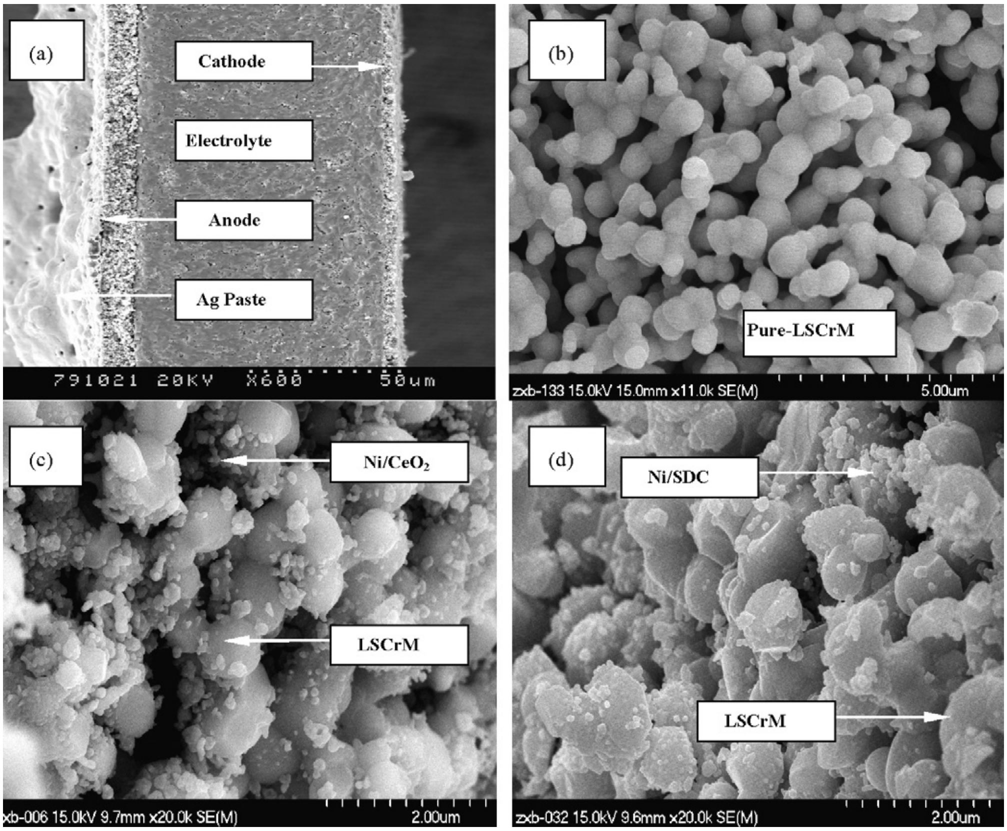

Fig. 4. SEM micrographs of the cross section of (a) the full cell and (b) pure-, (c) Ni/CeO_2- and (d) Ni/SDC-impregnated LSCrM anodes.

thickness and porosity of electrodes because there was no such obvious phenomenon occurring at high current densities with H_2 as fuel, as shown in Fig. 2(a). This may be explained because the catalytic ability of LSCrM + Ni-based anode is lower for the oxidation reaction of CH_4 than that of H_2 because the presence of Ni can effectively improve the oxidation reaction of the H_2 but not CH_4. Another reason may be the low conversion rate of methane. However, the exact reasons are not easy to confirm because of the complex reaction mechanism for CH_4, so further work needs to be done to clarify the mechanism.

Fig. 3 shows the impedance spectra of the LSCrM + Ni + CeO_2/YSZ/LSM + SDC cell for dry H_2 and CH_4 fuels. Clearly, the cell exhibits lower polarization resistance in H_2 compared with CH_4 at different temperatures. The impedance spectra in H_2 or CH_4 consist of at least two elements, which are typically characterized with a relative large arc in the low frequency range and a small arc in the high frequency range. The ohmic resistance corresponding to the high-frequency intercept of the arc usually consists of electrolyte resistance, contact resistance and electrode ohmic resistance. Fig. 3(a) shows a marked change with temperature for the high frequency element consisting of at least two small circles. At 850 °C there was about an 80% reduction compared with that at 700 °C. But for the low frequency element, being close to a semicircle, there was no significant change over this range of temperature. For the impedance spectra tested with CH_4, similar trends can be found, as shown in Fig. 3(b).

Fig. 4(a) shows the SEM micrograph of the cross section of the full cell taken after the fuel cell test. The thickness of electrolyte of the cell is 83 μm, effectively decreasing the electrolyte-ohmic resistance. Although there are still a few enclosed pores in the electrolyte support, they are separated from each other and cannot cause any gas leakage. The cathode is 5 μm thick and the anode is about 10 μm thick, covered with a thick layer of Ag current collector. For the pure-LSCrM anode shown in Fig. 4(b), the grain size of LSCrM is 0.5–1.0 μm and the grains form a clear network between the adjacent LSCrM particles, indicating a good interfacial contact between them. In the impregnated LSCrM anodes shown in Fig. 4(c) and (d), LSCrM particles formed the backbone of the anode with small particles of about 100 nm in diameter distributed around them. There is also an effective connection between the small particles and the LSCrM network, but the connections between the small particles filling the pores is bad. For this reason, the ionic conducting path in this anode is poor. So, besides the improvement of local oxygen ionic conduction, the enhancement of the anode performance should be mainly attributed to the improvement of the catalytic activity produced by feeding oxygen from the catalyst. In addition, the catalytic activity of SDC for hydrocarbon oxidation was lower than that of CeO_2 [18]. These two reasons may be used to explain why the values of P_{max} for SOFCs using anodes with the addition of Ni/CeO_2 are higher than those with the addition of Ni/SDC.

Compared to the pure-LSCrM anode, the porosity of the impregnated LSCrM anode is lower, which indicates that the anode performance could be further improved by optimization of the anode pore structure. Carbon deposits were not observed on the Ni-impregnated LSCrM anodes after operating with CH_4 fuel at 750–900 °C for 7 h operation, as confirmed by SEM in Fig. 4(c) and (d). This also shows that Ni/LSCrM is a composite anode which has great development potential.

4. Conclusion

YSZ electrolyte-supported SOFCs using one or more types of Ni, SDC and CeO_2 modified LSCrM anodes and an SDC modified LSM cathode were fabricated and tested. The results indicated that Ni and CeO_2 played an important role in the direct oxidation of methane. Pure CeO_2 showed a better catalytic activity for the oxidation reaction than SDC. Ni played a primary role in promoting the performance of the LSCrM-based anode. Further work is underway to investigate the effect of the Ni content on the cell performance.

Acknowledgement

The authors thank the Ministry of Science and Technology of China (contract no. 2007AA05Z139) for its financial support.

References

[1] Y. Matsuzaki, I. Yasuda, Solid State Ionics 132 (2000) 261–268.
[2] B.C.H. Steele, I. Kelly, H. Middleton, R. Rudkin, Solid State Ionics 28 (1988) 1547–1552.
[3] Z.F. Zhou, R. Kumar, S.T. Thakur, L.R. Rudnick, H. Schobert, S.N. Lvov, J. Power Sources 171 (2007) 856–860.
[4] X.L. Huang, H.L. Zhao, W.H. Qiu, W.J. Wu, X. Li, Energ. Convers. Manage. 48 (2007) 1678–1682.
[5] A.D. Lan, A.S. Mukasyan, J. Phys. Chem. C 111 (2007) 9573–9582.
[6] X.J. Chen, Q.L. Liu, S.H. Chan, N.P. Brandon, K.A. Khor, Electrochem. Commun. 9 (2007) 767–772.
[7] S.W. Tao, J.T.S. Irvine, Nat. Mater. 2 (2003) 320–325.
[8] S.W. Tao, J.T.S. Irvine, J. Electrochem. Soc. 151 (2004) A252–A257.
[9] J. Wan, J.H. Zhu, J.B. Goodenough, Solid State Ionics 177 (2006) 1211–1217.
[10] S.P. Jiang, X.J. Chen, S.H. Chan, J.T. Kwok, J. Electrochem. Soc. 153 (2006) A850–A856.
[11] J. Peña-Martínez, D. Marrero-López, D. Pérez-Coll, J.C. Ruiz-Morales, P. Núñez, Electrochim. Acta 52 (2007) 2950–2958.
[12] J. Liu, B.D. Madsen, Z.Q. Ji, S.A. Barnett, Electrochem, Solid-State Lett. 5 (2002) A122–A124.
[13] S.P. Jiang, Mater. Sci. Eng. A 418 (2006) 199–210.
[14] X.J. Chen, Q.L. Liu, K.A. Khor, S.H. Chan, J. Power Sources 165 (2007) 34–40.
[15] R. Su, Z. Lü, K.F. Chen, N. Ai, S.Y. Li, B. Wei, W.H. Su, Electrochem. Commun. 10 (2008) 844–847.
[16] J.B. Goodenough, Y.H. Huang, J. Power Sources 173 (2007) 1–10.
[17] W.Z. Zhu, S.C. Deevi, Mater. Sci. Eng. A 362 (2003) 228–239.
[18] H. Kurokawa, L.M. Yang, C.P. Jacobson, L.C.D. Jonghe, S.J. Visco, J. Power Sources 164 (2007) 510–518.
[19] M. Nolan, S.C. Parker, G.W. Watson, Surf. Sci. 595 (2005) 223–232.
[20] S. Zhao, R.J. Gorte, S.M. Plint, Appl. Catal. A-Gen. 227 (2004) 129–136.
[21] S.W. Tao, J.T.S. Irvine, S.M. Plint, J. Phys. Chem. B 110 (2006) 21771–21776.